

Received June 23, 2019, accepted July 22, 2019, date of publication July 29, 2019, date of current version August 20, 2019.

Digital Object Identifier 10.1109/ACCESS.2019.2931554

Characterizing Turbulence-Induced Decay of Mutual Unbiasedness of Complementary Bases Relevant to Propagated Photonic Spatial-Mode States

CHUNYI CHEN^{ID} AND HUAMIN YANG

Key Laboratory of Photoelectric Measurement & Control and Optical Information Transfer Technology, Changchun University of Science and Technology, Changchun 130022, China

Corresponding author: Chunyi Chen (chenchunyi@hotmail.com)

This work was supported in part by the National Science Foundation of China under Grant 61475025 and Grant 61775022 and in part by the Development Program of Science and Technology of Jilin Province of China under Grant 20180519012JH.

ABSTRACT Mutually complementary bases are crucial to secure quantum key distribution (QKD). By aiming at free-space QKD with use of spatially structured photons, the effect of turbulence on the mutual unbiasedness of two complementary bases relevant to photonic orbital-angular-momentum (OAM) modes is modeled theoretically, with novel insightful expressions and physical explanations yielded. For two complementary bases constructed from Laguerre–Gaussian (LG) modes with a fixed radial index of zero, it is shown that the superposed joint-two-LG-mode (JTLGM) correlation function plays a fundamental role in determining the turbulence-induced mutual-unbiasedness decay. The mutual information between the sent and detected photonic states is used as a metric to quantify the degree of turbulence-induced mutual-unbiasedness decay. It is found that the degree of turbulence-induced mutual-unbiasedness decay depends on the scaled atmospheric coherence width, anisotropy of turbulence and contents of the complementary bases, and it can become non-negligible in certain cases.

INDEX TERMS Mutual unbiasedness, complementary bases, photonic spatial-mode state, quantum key distribution, atmospheric turbulence, anisotropy.

I. INTRODUCTION

Over the years, quantum key distribution (QKD) has become one of the important research fronts in the area of quantum information science and technology. Traditional QKD schemes generally employ qubits, i.e., two-dimensional quantum systems, for encoding information. However, recently higher-dimensional QKD schemes have also been experimentally demonstrated by utilizing the photonic spatial degrees of freedom. For instance, twisted photons carrying orbital angular momentum (OAM) have been treated as alphabets in experiments of QKD with qudits [1]–[3]. Indeed, photonic OAM-mode states with various quantum numbers span a discrete infinite-dimensional Hilbert space and are a good option for implementing qudits. Secure QKD protocols, irrespective of using qubits or qudits, necessitate

complementary bases, i.e., the mutually unbiased bases [2]. For QKD with use of photonic spatial degrees of freedom, a specific set of photonic OAM-mode states can be utilized as a primary encoding basis, which we designate as the standard basis for later ease of description, and its complementary bases can be further yielded by performing proper linear combination of the photonic OAM-mode states [1], [2]. An approach to constructing a d -dimensional basis mutually unbiased with respect to a standard basis in dimension d is to adopt the following superposition of all the elements in the standard basis [4]

$$|\psi_n\rangle = \frac{1}{\sqrt{d}} \sum_{m=0}^{d-1} \exp\left(\frac{i 2\pi nm}{d}\right) |\phi_m\rangle, \quad (1)$$

where $|\phi_m\rangle$ denotes the m^{th} element in the standard basis, and $n \in \{0, 1, \dots, d-1\}$. Here and hereafter, Dirac's "bracket" notation is used to describe an element in a photonic

The associate editor coordinating the review of this manuscript and approving it for publication was Nianqiang Li.

state basis in an abstract manner. For later convenience of description, from now on, we refer to the d -dimensional basis $\{|\psi_n\rangle\}$ defined by (1) as the Hadamard basis.

The said standard and Hadamard bases are two complementary bases and can keep mutually unbiased upon propagation in vacuum [1]; this nature is crucial to effective recognition of an attack in QKD applications [4]. On the other hand, it is known that when QKD with use of spatially structured photons is operated in free-space optical channels through the earth’s atmosphere, turbulence therein will distort the propagating photonic wave fields, hence disturbing the propagated photonic spatial-mode states. With this in mind, a natural problem that then arises is how atmospheric turbulence affects the mutual unbiasedness of complementary bases relevant to propagated photonic spatial-mode states. However, to our best knowledge, there are, up to now, very few published works with respect to the problem. This may seem quite surprising if one recalls how much effort has already been put into examination of turbulence-induced OAM intermodal crosstalk in both quantum and classical contexts (see, e.g., [5]–[10]). Unlike these existing researches, our work is intended to fill the deficiency in the understanding of changes in the mutual unbiasedness of complementary bases associated with photonic spatial-mode states propagating through atmospheric turbulence.

In what follows, we first theoretically formulate, in Section II, the average probability of detecting a photon, initially prepared in the Hadamard basis, by using the standard basis as the measurement basis in the presence of turbulence-caused distortion. With the help of the developed formulae, we subsequently quantify, in Section III, the turbulence-induced mutual-unbiasedness decay of the standard and Hadamard bases by using the mutual information between the sent and detected photonic states as a metric. Finally, conclusions are drawn in Section IV.

II. AVERAGE PROBABILITY OF DETECTING A PHOTON PREPARED IN HADAMARD BASIS WITH STANDARD BASIS USED AS MEASUREMENT BASIS

Here we assume that a photon associated with a spatial-mode state in a d -dimensional Hadamard basis propagates along the positive z -axis from the transmitting plane at $z = 0$ to the receiving plane at $z = L$. The coordinate-space wave function of the photonic state at the receiving plane can be explicitly expressed by

$$\psi_n^{(L)}(\mathbf{r}) \triangleq \langle \mathbf{r} | \psi_n \rangle = \frac{1}{\sqrt{d}} \sum_{m=0}^{d-1} \exp\left(\frac{i 2\pi nm}{d}\right) \phi_m^{(L)}(\mathbf{r}), \quad (2)$$

where $\mathbf{r} = (r, \theta_r)$ represents a two-dimensional position vector in the receiving plane,

$$\phi_m^{(L)}(\mathbf{r}) = \langle \mathbf{r} | \phi_m \rangle = R^{(m)}(r, L) \exp(i l_m \theta_r) / (2\pi)^{1/2}, \quad (3)$$

and the superscript “ L ” in parentheses indicates the dependence of the associated quantity on the parameter L ; $\langle \mathbf{r} |$ is the “bra” vector that corresponds to the “ket” vector $|\mathbf{r}\rangle$,

which is an element in the spatial coordinate basis related to a two-dimensional plane; $R^{(m)}(r, L)$ is the radially-dependent part of the coordinate-space wave function of the state $|\phi_m\rangle$ and $\int_0^\infty |R^{(m)}(r, L)|^2 r dr = 1$; l_m is the OAM index of the state $|\phi_m\rangle$. In this paper, we always use the lowercase letter “ l ” with a subscript to denote the OAM index of a state in the standard basis, and the subscript represents the basis index associated with the state. This notation usage will be utilized later without further explicit explanation. Here we emphasize that, despite the one-to-one correspondence between the OAM index l_m and the basis index m , l_m may take on a value different from that of m . We note that, except for plane or spherical waves, it is often very difficult to develop insightful mathematical expressions for fluctuation statistics of optical waves propagating in moderate-to-strong atmospheric turbulence. Furthermore, free-space QKD systems with use of spatially structured photons may not work normally under moderate-to-strong turbulence conditions. Thus, in what follows, we confine our consideration to weak-turbulence cases; more specifically, the role of turbulence is reasonably modeled by a single phase screen. It is noted that many researchers [5], [8]–[12] have done theoretical studies of optical OAM-mode propagation in turbulence under this consideration. In addition, numerous experimental demonstrations relevant to optical OAM transmission [13]–[15] have also used a single phase screen displayed by a spatial light modulator to simulate the turbulence-induced distortion in laboratory.

The mutually unbiased relation between the aforementioned standard and Hadamard bases implies $|\langle \phi_m | \psi_n \rangle|^2 = 1/d$ for $\forall m, n \in \{0, 1, \dots, d - 1\}$ in the absence of turbulence. When there is turbulence distortion along the propagation path, the pure state $|\psi_n\rangle$ evolves into a new superposed state $|\psi_{n,tur}\rangle$ with its coordinate-space wave function given by

$$\psi_{n,tur}^{(L)}(\mathbf{r}) = \frac{1}{\sqrt{d}} \sum_{m=0}^{d-1} \left\{ \phi_m^{(L)}(\mathbf{r}) \exp\left[i \frac{2\pi nm}{d} + i\varphi(\mathbf{r}, L) \right] \right\} \quad (4)$$

for a given random turbulence realization, where $\varphi(\mathbf{r}, L)$ denotes the phase perturbation induced by the turbulence realization, which is physically represented via a random phase screen thereafter. If we carry out projective measurement of the photon associated with the state $|\psi_{n,tur}\rangle$ for a given turbulence realization in the d -dimensional standard basis at the receiving plane, the probability of finding the photon in the state $|\phi_m\rangle$ ($m \in \{0, 1, \dots, d - 1\}$) can be formulated by

$$p_{m|n} = |\langle \phi_m | \psi_{n,tur} \rangle|^2 = |a_{m,n}|^2 = a_{m,n} a_{m,n}^*, \quad (5)$$

where the asterisk denotes the complex conjugate, and

$$a_{m,n} = \int \int_{-\infty}^{\infty} \psi_{n,tur}^{(L)}(\mathbf{r}) \phi_m^{(L)*}(\mathbf{r}) d^2\mathbf{r}. \quad (6)$$

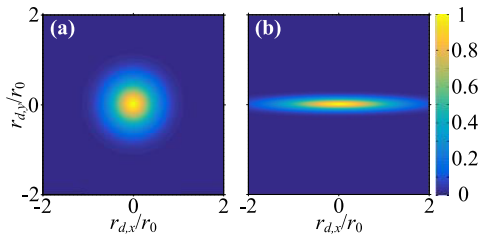


FIGURE 1. Distribution pattern of the weighting factor $\exp[-D_\varphi(\mathbf{r}_d)/2]$ with different ζ_e , where $\mathbf{r}_d = (r_{d,x}, r_{d,y})$, $\alpha = 11/3$, $r_0 = 5$ cm. (a) $\zeta_e = 1$; (b) $\zeta_e = 10$.

The ensemble average of $p_{m|n}$ over different random turbulence realizations is found to be

$$\bar{p}_{m|n} = \langle a_{m,n} a_{m,n}^* \rangle_{\text{tur}}, \quad (7)$$

where $\langle \cdot \rangle_{\text{tur}}$ stands for the ensemble averaging operation over the statistics of atmospheric turbulence.

To evaluate $\bar{p}_{m|n}$, one needs to specify the spatial power spectrum of refractive-index fluctuations for the atmospheric turbulence. Statistical isotropy has been often considered valid for turbulence in the atmosphere. However, there are experimental observations demonstrating the existence of statistical anisotropy of the turbulence in some portions of the atmosphere (see, e.g., [16], [17]). It has been shown that the anisotropy of the turbulence has an important impact on optical-wave propagation [18], [19]. In fact, the wave field of the spatial-mode states in the Hadamard basis may feature a non-circularly-symmetric pattern, viz., may exhibit obvious direction-dependence (see, e.g., Fig. 1 in [2]). This may arouse one’s curiosity about whether anisotropy of turbulence plays a role in decaying the mutual unbiasedness of complementary bases relevant to propagated photonic spatial-mode states. To deal with this issue, below we choose a turbulence spectrum taking the following form [18]

$$\Phi_n(\mathbf{K}) = A(\alpha) \tilde{C}_n^2 \zeta_e^2 \left(\zeta_e^2 \kappa_x^2 + \kappa_y^2 + \zeta_e^2 \kappa_z^2 \right)^{-\alpha/2}, \quad (8)$$

where $\mathbf{K} = (\kappa_x, \kappa_y, \kappa_z)$ is the vector wave number, $A(\alpha) = \Gamma(\alpha-1)\cos(\alpha\pi/2)/(4\pi^2)$, $\Gamma(\cdot)$ represents the gamma function, ζ_e denotes the effective anisotropy factor, α is the spectral index, $3 < \alpha < 4$, and \tilde{C}_n^2 is the generalized refractive-index structure constant in units of $\text{m}^{3-\alpha}$. We point out that the above spectrum is obtained from (20) in [18] by assuming an inner scale l_0 of zero and an outer scale L_0 of infinity for the turbulence whose anisotropy exists in planes perpendicular to the z -axis, i.e., the propagation axis. The turbulence spectrum with $l_0 \rightarrow 0$ and $L_0 \rightarrow \infty$ is proper for many cases and used widely in the literature [3], [10], [11]. Incidentally, the above spectrum becomes isotropic if $\zeta_e = 1$ and reduces to the canonical Kolmogorov spectrum if $\alpha = 11/3$.

To proceed further, here we use a set of Laguerre-Gaussian (LG) spatial modes with a fixed radial index of zero to construct the standard basis relevant to photonic OAM-mode

states, implying that $R^{(m)}(r, L)$ appearing in $\phi_m^{(L)}(\mathbf{r})$ should be expressed by [20], [21]

$$R^{(m)}(r, L) = \frac{2}{w_L} \sqrt{\frac{1}{(l_m)!}} \left(\frac{r\sqrt{2}}{w_L} \right)^{|l_m|} \exp(-i\Theta) \times \exp \left[-\frac{r^2}{w_L^2} + \frac{ikr^2L}{2(L^2 + z_R^2)} \right], \quad (9)$$

where k is the optical wavenumber, $\Theta = (|l_m| + 1) \arctan(L/z_R)$ is the Gouy phase, $z_R = kw_0^2/2$ is the Rayleigh range, $w_L = w_0[(L^2 + z_R^2)/z_R^2]^{1/2}$ is the fundamental-Gaussian-beam radius at the receiving plane, and w_0 represents the beam-waist radius of a fundamental-Gaussian-beam field; for ease of description, later we also denote the mode $\phi_m^{(L)}(\mathbf{r})$ by $\text{LG}_0^{l_m}$. Substitution of (6) into (7) leads to

$$\bar{p}_{m|n} = \frac{1}{d} \sum_{s_1=0}^{d-1} \sum_{s_2=0}^{d-1} \exp \left[i \frac{2\pi n (s_1 - s_2)}{d} \right] \iint_{-\infty}^{\infty} d^2\mathbf{r}_1 \times \iint_{-\infty}^{\infty} d^2\mathbf{r}_2 U_{s_1}^{(m)}(\mathbf{r}_1) U_{s_2}^{(m)*}(\mathbf{r}_2) M(\mathbf{r}_1, \mathbf{r}_2), \quad (10)$$

where

$$U_s^{(m)}(\mathbf{x}) = \phi_s^{(L)}(\mathbf{x}) \phi_m^{(L)*}(\mathbf{x}), \quad (11)$$

$$M(\mathbf{r}_1, \mathbf{r}_2) = \langle \exp[i\varphi(\mathbf{r}_1, L) - i\varphi(\mathbf{r}_2, L)] \rangle_{\text{tur}} = \exp[-D_\varphi(\mathbf{r}_1 - \mathbf{r}_2)/2], \quad (12)$$

$D_\varphi(\mathbf{x})$ with \mathbf{x} being a two-dimensional column vector represents the structure function of the random phase screen $\varphi(\mathbf{r}, L)$. We note that $U_s^{(m)}(\cdot)$ stands for a joint two-LG-mode (JTLGM) field defined as the product of the mode $\text{LG}_0^{l_s}$ and the complex conjugate of the mode $\text{LG}_0^{l_m}$. In arriving at the second step of (12), it is assumed that $\varphi(\mathbf{r}, L)$ is a Gaussian random process. For atmospheric turbulence statistically modeled by (8), it follows that [18]

$$D_\varphi(\mathbf{x}) = 2 \times \left[2.1 \zeta_e^{1/(\alpha-2)} |\mathbf{I}_a \mathbf{x}| / r_0 \right]^{\alpha-2}, \quad (13)$$

where $r_0 = 2.1\rho_{\text{pl}}$ is the Fried’s plane-wave atmospheric coherence width, $\rho_{\text{pl}} = [-2^{3-\alpha}\pi^2\Gamma(1-\alpha/2)A(\alpha)\tilde{C}_n^2 L k^2 / \Gamma(\alpha/2)]^{1/(2-\alpha)}$, and

$$\mathbf{I}_a = \begin{bmatrix} \zeta_e^{-1} & 0 \\ 0 & 1 \end{bmatrix}. \quad (14)$$

By making the change of variables $\mathbf{R} = (\mathbf{r}_1 + \mathbf{r}_2)/2$ and $\mathbf{r}_d = \mathbf{r}_1 - \mathbf{r}_2$, (10) can be rewritten as follows:

$$\bar{p}_{m|n} = \frac{1}{d} \sum_{s_1=0}^{d-1} \sum_{s_2=0}^{d-1} \exp \left[i \frac{2\pi n (s_1 - s_2)}{d} \right] \iint_{-\infty}^{\infty} d^2\mathbf{r}_d \times \exp[-D_\varphi(\mathbf{r}_d)/2] \iint_{-\infty}^{\infty} d^2\mathbf{R} U_{s_1}^{(m)}\left(\mathbf{R} + \frac{\mathbf{r}_d}{2}\right) \times U_{s_2}^{(m)*}\left(\mathbf{R} - \frac{\mathbf{r}_d}{2}\right). \quad (15)$$

If we further let $\mathbf{R}' = \mathbf{R} + \mathbf{r}_d/2$ in (15), it is easy to find that the integration over \mathbf{R}' therein is actually equivalent to

the two-dimensional correlation integral between $U_{s_1}^{(m)}(\cdot)$ and $U_{s_2}^{(m)}(\cdot)$. With this in mind, one can obtain

$$\bar{p}_{m|n} = \frac{1}{d} \iint_{-\infty}^{\infty} \exp[-D_\varphi(\mathbf{r}_d)/2] \Lambda_n^{(m)}(\mathbf{r}_d) d^2\mathbf{r}_d, \quad (16)$$

where

$$\Lambda_n^{(m)}(\mathbf{r}_d) = \sum_{s_1=0}^{d-1} \sum_{s_2=0}^{d-1} \left\{ \gamma_{s_1, s_2}^{(m)}(\mathbf{r}_d) \exp[i 2\pi n (s_1 - s_2) / d] \right\}, \quad (17)$$

$$\gamma_{s_1, s_2}^{(m)}(\mathbf{x}) = F^{-1} \left\{ \tilde{U}_{s_1}^{(m)}(\boldsymbol{\kappa}) \tilde{U}_{s_2}^{(m)*}(\boldsymbol{\kappa}) \right\}, \quad (18)$$

$\tilde{U}_s^{(m)}(\boldsymbol{\kappa}) = F \left[U_s^{(m)}(\mathbf{x}) \right]$, and $\boldsymbol{\kappa} = (\kappa, \theta_\kappa)$ represents the spatial circular frequency vector; F and F^{-1} denote the Fourier transform and inverse Fourier transform, respectively. We emphasize once again that $\gamma_{s_1, s_2}^{(m)}(\cdot)$ is obtained by employing the correlation theorem and actually denotes the correlation function between $U_{s_1}^{(m)}(\cdot)$ and $U_{s_2}^{(m)}(\cdot)$. Note that, $\Lambda_n^{(m)}(\cdot)$ is a linear superposition of various $\gamma_{s_1, s_2}^{(m)}(\cdot)$; hence, later we will refer to it as the superposed JTLGM correlation function. In accordance with the asymmetric form of the Fourier transform [22], based on (3), (9) and (11), the expression for the Fourier transform of $U_s^{(m)}(\cdot)$ can be developed to give

$$\begin{aligned} \tilde{U}_s^{(m)}(\boldsymbol{\kappa}) &= \frac{\pi C_s^{(m)} [\text{sgn}(l_s - l_m)]^{l_s - l_m}}{i^{l_s - l_m} (|l_s - l_m|)!} \left(\frac{w_L}{\sqrt{2}} \right)^{|l_s| + |l_m| + |l_s - l_m| + 2} \left(\frac{\kappa}{2} \right)^{|l_s - l_m|} \\ &\times {}_1F_1 \left[\frac{|l_s - l_m| + |l_s| + |l_m| + 2}{2}, |l_s - l_m| + 1, - \left(\frac{w_L \kappa}{2\sqrt{2}} \right)^2 \right] \\ &\times \Gamma \left(\frac{|l_s - l_m| + |l_s| + |l_m| + 2}{2} \right) \exp[i (l_s - l_m) \theta_\kappa], \end{aligned} \quad (19)$$

where ${}_1F_1(\cdot)$ is the confluent hypergeometric function of the first kind, $\text{sgn}(\cdot)$ is the signum function, and

$$C_s^{(m)} = \frac{1}{\sqrt{\pi^2 (|l_s|)! (|l_m|)!}} \left(\frac{2}{w_L^2} \right)^{(|l_s| + |l_m|)/2 + 1} \times \exp[-i (|l_s| - |l_m|) \arctan(L/z_R)]. \quad (20)$$

When $l_s \equiv l_m \equiv 0$, one finds that $U_s^{(m)}(\mathbf{x}) = 2(\pi w_L^2)^{-1} \exp(-2|\mathbf{x}|^2/w_L^2)$ and $\tilde{U}_s^{(m)}(\boldsymbol{\kappa}) = \exp(-w_L^2 \kappa^2/8)$. Hence, it is easy to verify that (19) is certainly the Fourier transform of $U_s^{(m)}(\mathbf{x})$ if both l_s and l_m are equal to zero. For other cases, we have verified (19) by comparing the results calculated according to it with those computed via a fast-Fourier-transform (FFT) algorithm. With the help of (19), it is straightforward to calculate $\gamma_{s_1, s_2}^{(m)}(\cdot)$ by using an inverse FFT algorithm.

Equations (16) – (19) show one of our theoretical contributions in this work. According to (16), it is noted that $\bar{p}_{m|n}$ is simply a weighted integration of the superposed JTLGM correlation function with the turbulence-related term $\exp[-D_\varphi(\mathbf{r}_d)/2]$ acting as a weighting factor. Furthermore, it is easy to find from (17) and (18) that, for given standard and

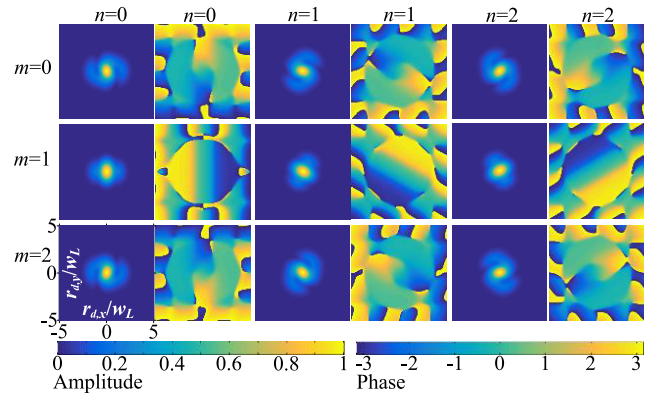


FIGURE 2. Amplitude and phase patterns of various $\Lambda_n^{(m)}(\mathbf{r}_d)$, where $\mathbf{r}_d = (r_{d,x}, r_{d,y})$, $L = 5$ km, $w_0 = 5$ cm, and $k = 2\pi/\lambda$ with $\lambda = 800$ nm. The standard basis comprises $\{\text{LG}_0^{-1}, \text{LG}_0^0, \text{LG}_0^1\}$. The first, third, and fifth columns correspond to the amplitude scaled by $\Lambda_n^{(m)}(\mathbf{0})$; the second, fourth, and sixth columns correspond to the phase.

Hadamard bases, the superposed JTLGM correlation function is completely determined by the basis indices m and n , irrespective of atmospheric turbulence. The role of turbulence distortion in examination of the mutual-unbiasedness relation between the standard and Hadamard bases is completely played by the weighting factor, which is equal to 1 if there is no turbulence, i.e., if $r_0 \rightarrow \infty$. Fig. 1 illustrates the weighting factor with various effective anisotropy factor ζ_e . It is seen from Fig. 1 that ζ_e determines the shape of the weighting factor's distribution pattern; specifically, the weighting factor possesses a circle- and ellipse-shaped distribution pattern, respectively, when $\zeta_e = 1$ and 10. The physical explanation of this behavior is as follows: $\zeta_e \neq 1$ means the turbulence is anisotropic, resulting in that the weighting factor's distribution pattern has different scale sizes in the x and y directions. In addition, it is easy to infer that, with fixed ζ_e , the scale size of the weighting factor's distribution pattern is completely determined by r_0 , and a larger r_0 induces a distribution pattern with a greater scale size. The said properties of the weighting factor produce important effects on the decay of the mutual unbiasedness of the standard and Hadamard bases, which will be further elucidated in the following.

Now we examine the characteristics of the superposed JTLGM correlation function $\Lambda_n^{(m)}(\mathbf{r}_d)$. Figs. 2 and 3 exemplify the amplitude and phase patterns of various superposed JTLGM correlation functions. It is found by comparing Figs. 2 and 3 that the content of the standard basis has a significant impact on $\Lambda_n^{(m)}(\mathbf{r}_d)$. Standard bases consisting of different OAM-mode-state elements lead to different amplitude and phase patterns of the superposed JTLGM correlation function. Moreover, it is straightforward to find from Figs. 2 and 3 that, even with the same standard basis, $\Lambda_n^{(m)}(\mathbf{r}_d)$ may vary with changing m ; indeed, $\Lambda_n^{(0)}(\mathbf{r}_d) \neq \Lambda_n^{(1)}(\mathbf{r}_d) \neq \Lambda_n^{(2)}(\mathbf{r}_d)$ for the cases of both Figs. 2 and 3. Nevertheless, with a given standard basis, it can be proved that

$$\iint_{-\infty}^{\infty} \Lambda_n^{(m)}(\mathbf{r}_d) d^2\mathbf{r}_d \equiv 1 \quad (21)$$

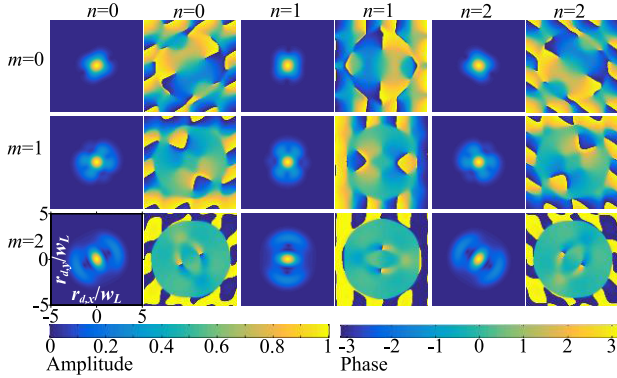


FIGURE 3. Amplitude and phase patterns of various $\Lambda_n^{(m)}(\mathbf{r}_d)$, where $\mathbf{r}_d = (r_{d,x}, r_{d,y})$, $L = 5$ km, $w_0 = 5$ cm, and $k = 2\pi/\lambda$ with $\lambda = 800$ nm. The standard basis comprises $\{LC_0^0, LG_0^1, LC_0^2\}$. The first, third, and fifth columns correspond to the amplitude scaled by $\Lambda_n^{(m)}(\mathbf{0})$; the second, fourth, and sixth columns correspond to the phase.

for $\forall m \in \{0, 1, \dots, d-1\}$, which is consistent with the fact that the standard and Hadamard bases are mutually unbiased in the absence of turbulence. Further, $\Lambda_n^{(m)}(\mathbf{r}_d)$ is often complex-valued, whereas one can find that

$$\Lambda_n^{(m)}(\mathbf{0}) = \sum_{s=0}^{d-1} \gamma_{s,s}^{(m)}(\mathbf{0}) \quad (22)$$

is real-valued with

$$\gamma_{s,s}^{(m)}(\mathbf{0}) = (2\pi)^{-1} \int_0^\infty r |R^{(m)}(r, L)R^{(s)}(r, L)|^2 dr. \quad (23)$$

We point out that (22) is obtained by recognizing that $\gamma_{s_1, s_2}^{(m)}(\mathbf{0}) \equiv 0$ if $s_1 \neq s_2$.

Indeed, the aforementioned weighting factor $\exp[-D_\varphi(\mathbf{r}_d)/2]$ plays a role of changing the spatial structure of $\Lambda_n^{(m)}(\mathbf{r}_d)$ in evaluation of the integration in (16); evidently, the resultant degree of change in the spatial structure of $\Lambda_n^{(m)}(\mathbf{r}_d)$ depends on two factors: one is the relative scale sizes of the distribution pattern of $\exp[-D_\varphi(\mathbf{r}_d)/2]$ and the amplitude pattern of $\Lambda_n^{(m)}(\mathbf{r}_d)$; the other is the variation behavior of $\Lambda_n^{(m)}(\mathbf{r}_d)$ with changing \mathbf{r}_d . By keeping these in mind, one can infer that $\bar{p}_{m|n}$ may take on a value different from that of $\bar{p}_{m'|n}$ if $\Lambda_n^{(m)}(\mathbf{r}_d)$ and $\Lambda_n^{(m')}(\mathbf{r}_d)$ have different spatial variation behavior, and hence the weighting factor $\exp[-D_\varphi(\mathbf{r}_d)/2]$ causes different changes in the spatial structure of $\Lambda_n^{(m)}(\mathbf{r}_d)$ and $\Lambda_n^{(m')}(\mathbf{r}_d)$. This implies that when a photon initially prepared in the n^{th} spatial-mode state of the Hadamard basis is propagated via atmospheric turbulence, the average probability of finding the photon in the m^{th} OAM-mode state of the standard basis may be different from that of finding the photon in the m'^{th} OAM-mode state of the standard basis; in other words, the mutual unbiasedness of the standard and Hadamard bases is somewhat decayed by the turbulence. Based on the above analysis, the most fundamental reason for the mutual-unbiasedness decay is that, for a given propagated photon initially in a spatial-mode state of the Hadamard basis, various state elements in the measurement basis, here namely

the standard basis, correspond to superposed JTLGM correlation functions that may possess different spatial-structure features due to the dependence of the JTLGM fields on the measurement basis index m .

As a comment, here we point out that LG modes are characterized by both their OAM index (i.e., azimuthal index) and their radial index. Theoretically speaking, the said standard basis can also be constructed by using a set of LG modes with a fixed OAM index and different radial indices. In fact, (16)–(18) remain valid for a standard basis consisting of LG modes with a fixed OAM index and different radial indices. Of course, (19) is only applicable to a standard basis comprising various LG modes with a fixed radial index of zero. Because published reports concerning QKD with use of spatially structured photons [3], [12], [14], [15] have widely considered the cases of employing LG modes with a fixed radial index of zero to construct the standard basis, we only deal with, in this paper, the standard bases comprising LG modes described by (3) and (9).

III. QUANTIFICATION OF TURBULENCE-INDUCED MUTUAL-UNBIASEDNESS DECAY OF STANDARD AND HADAMARD BASES

To quantify the turbulence-caused decay of mutual unbiasedness of the standard and Hadamard bases, in this section we examine the mutual information between the sent and detected photonic states, given by

$$I_{HS} = \sum_{n=0}^{d-1} \left[P_{H,n} \sum_{m=0}^{d-1} (P_{m|n} \log_2 P_{m|n}) \right] - \sum_{m=0}^{d-1} (P_{S,m} \log_2 P_{S,m}), \quad (24)$$

where $P_{H,n}$ denotes the probability of sending a photon in the state $|\psi_n\rangle$, $P_{m|n}$ represents the conditional probability of detecting a photon in the state $|\phi_m\rangle$ given a sent photon in the state $|\psi_n\rangle$, and

$$P_{S,m} = \sum_{n=0}^{d-1} P_{m|n} P_{H,n}. \quad (25)$$

It is known that turbulence-induced random scattering may transform propagated photons out of the spatial-mode measurement basis, resulting in a null event in the detection output, which causes $\sum_{m=0}^{d-1} \bar{p}_{m|n} < 1$. In QKD applications, time frames with the said null event are eliminated in the procedure of basis reconciliation. For this reason, below we let

$$P_{m|n} = \bar{p}_{m|n} / \sum_{m'=0}^{d-1} \bar{p}_{m'|n}. \quad (26)$$

To facilitate the subsequent analysis, we suppose a uniform probability for sending d states of the Hadamard basis, i.e., $P_{H,n} \equiv 1/d$. It is evident that $I_{HS} = 0$ in the absence of turbulence. The magnitude of I_{HS} quantitatively characterizes the degree of mutual-unbiasedness decay of the standard and Hadamard bases.

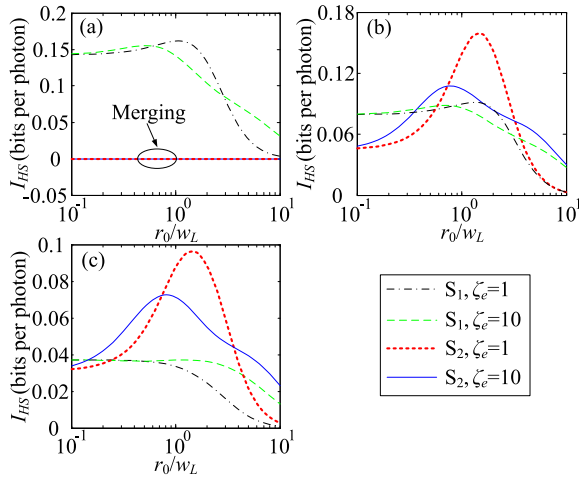


FIGURE 4. I_{HS} in terms of r_0/w_L with various ζ_e , where $L = 5$ km, $w_0 = 5$ cm, and $k = 2\pi/\lambda$ with $\lambda = 800$ nm; S_1 and S_2 in the legend denote different standard bases. (a) $S_1 = \{LG_0^{-2}, LG_0^2\}$ and $S_2 = \{LG_0^{-2}, LG_0^2\}$; (b) $S_1 = \{LG_0^0, LG_0^1, LG_0^3\}$ and $S_2 = \{LG_0^{-3}, LG_0^0, LG_0^3\}$; (c) $S_1 = \{LG_0^0, LG_0^1, LG_0^2, LG_0^3\}$ and $S_2 = \{LG_0^{-4}, LG_0^{-1}, LG_0^1, LG_0^4\}$.

We note that the mutual information has been treated in the existing literature (see, e.g., [10], [23]) for understanding the channel capacity of OAM-photon-based communications. However, it should be emphasized that the mutual information given by (24) is different from that dealt with by [10], [23]; specifically, (24) is used to calculate the mutual information for the cases where photons initially prepared in the Hadamard basis are eventually measured in the standard basis, whereas the authors of [10], [23] did not consider this kind of preparation and measurement of photons.

Fig. 4 illustrates the variation behavior of I_{HS} under different conditions. Examination of Fig. 4 reveals that the degree of mutual-unbiasedness decay has dependence on the scaled atmospheric coherence width r_0/w_L , effective anisotropy factor ζ_e and the specific LG modes chosen for a standard basis, and can become non-negligible under certain conditions, in which I_{HS} may grow larger than 0.1 bits per photon. It is seen from Fig. 4(a) that $I_{HS} \equiv 0$ for the case of the standard basis $\{LG_0^{-2}, LG_0^2\}$. The underlying reason for this fact is that $\Lambda_n^{(0)}(\mathbf{r}_d) \equiv \Lambda_n^{(1)}(\mathbf{r}_d)$ for a two-dimensional standard basis $\{LG_0^{-l}, LG_0^l\}$ with any nonzero integer l . For a given standard basis, when r_0 is small enough, viz., the peak of the term $\exp[-D_\varphi(\mathbf{r}_d)/2]$, centered at $\mathbf{r}_d = \mathbf{0}$, is so sharp that $\Lambda_n^{(m)}(\mathbf{r}_d)$ does not change appreciably within the region where $\exp[-D_\varphi(\mathbf{r}_d)/2]$ takes on a nontrivial value, it follows that

$$\bar{P}_{m|n} \sim \frac{1}{d} \Lambda_n^{(m)}(\mathbf{0}) \iint_{-\infty}^{\infty} \exp[-D_\varphi(\mathbf{r}_d)/2] d^2\mathbf{r}_d. \quad (27)$$

As a result, when r_0 is small enough,

$$P_{m|n} \sim \Lambda_n^{(m)}(\mathbf{0}) / \sum_{m'=0}^{d-1} \Lambda_n^{(m')}(\mathbf{0}), \quad (28)$$

regardless of the turbulence parameters. This is the fundamental reason why two curves related to the same standard

basis in Fig. 4 gradually merge together and approach a specific value when r_0/w_L decreases below a small enough level. Although, as can be seen in Fig. 4, the asymptotic values of I_{HS} with r_0/w_L tending to zero under many conditions are nonzero, it is apparent that I_{HS} necessarily approaches zero when r_0/w_L tends to infinity, i.e., the turbulence vanishes. It is seen from Fig. 4 that the curves except those associated with S_2 in the subplot (a) and S_1 in the subplot (c) have a noticeable peak within the range $[0.3, 2]$ of r_0/w_L ; hence, the degree of mutual-unbiasedness decay does not necessarily enlarge monotonically with increasing turbulence-caused phase distortion. Additionally, one finds from Fig. 4 that ζ_e has a complicated impact on I_{HS} and whether increasing ζ_e enlarges the degree of mutual-unbiasedness decay depends largely on the specific value of r_0/w_L .

As a final comment, because we have considered hitherto only the cases where photons are initially prepared in the Hadamard basis and eventually measured in the standard one, it is unclear whether our previous formulae are applicable to those cases where photons are initially prepared in the standard basis and eventually measured in the Hadamard one. In what follows, we briefly address this issue. Similar to the preceding treatment, the coordinate-space wave function at the receiving plane for a photon initially prepared in the standard basis in the presence of turbulence-caused distortion can be expressed by

$$\phi_{m, \text{tur}}^{(L)}(\mathbf{r}) = \phi_m^{(L)}(\mathbf{r}) \exp[i\varphi(\mathbf{r}, L)], \quad (29)$$

where the subscript $m \in \{0, 1, \dots, d-1\}$ denotes the standard basis index. Following a procedure analogous to that used to derive (10), the average probability of finding the photon in the state $|\psi_n\rangle$ (the Hadamard basis index $n \in \{0, 1, \dots, d-1\}$) can be developed to give

$$\begin{aligned} \bar{P}_{n|m} = & \frac{1}{d} \sum_{s_1=0}^{d-1} \sum_{s_2=0}^{d-1} \exp\left[i \frac{2\pi n(s_1-s_2)}{d}\right] \int_{-\infty}^{\infty} d^2\mathbf{r}_1 \\ & \times \iint_{-\infty}^{\infty} d^2\mathbf{r}_2 U_{s_1}^{(m)}(\mathbf{r}_1) U_{s_2}^{(m)*}(\mathbf{r}_2) M(\mathbf{r}_2, \mathbf{r}_1). \quad (30) \end{aligned}$$

The only difference between (10) and (30) exists in the term $M(\cdot)$; more specifically, (10) contains $M(\mathbf{r}_1, \mathbf{r}_2)$, whereas (30) involves $M(\mathbf{r}_2, \mathbf{r}_1)$. Nevertheless, it is noted that $M(\mathbf{r}_1, \mathbf{r}_2)$ is actually equal to $M(\mathbf{r}_2, \mathbf{r}_1)$ due to the mathematical forms shown by (12) and (13). Hence, it is evident that $\bar{P}_{m|n} \equiv \bar{P}_{n|m}$ for $\forall m, n \in \{0, 1, \dots, d-1\}$. With this in mind, we can infer that our previous results can certainly be applied to the cases where the standard and Hadamard bases are used as the preparation and measurement bases, respectively.

IV. CONCLUSION

In this paper, by focusing on free-space QKD with use of spatially structured photons and taking the turbulence-induced distortion into account, the average probability of detecting a photon initially prepared in a given basis and eventually measured in its complementary basis is formulated analytically;

it is simply an integration of the superposed JTLGM correlation function weighted by the factor $\exp[-D_\varphi(\mathbf{r}_d)/2]$ for two complementary bases relevant to photonic OAM-mode states. Based on the obtained formulations, the decay of the mutual unbiasedness of two complementary bases relevant to photonic OAM-mode states propagating in atmospheric turbulence has been analyzed theoretically, and the degree of mutual-unbiasedness decay has been quantified by using the mutual information between the sent and detected photonic states as a metric. It was found that the scaled atmospheric coherence width, effective turbulence-anisotropy factor and specific contents of the bases play a crucial role in determining the degree of mutual-unbiasedness decay, which may become non-negligible under certain conditions. Our results are useful for examining the security aspect of QKD with spatially structured photons operated in atmospheric free-space optical channels.

REFERENCES

- [1] M. Mirhosseini, O. S. Magaña-Loaiza, M. N. O'Sullivan, B. Rodenburg, M. Malik, M. P. J. Lavery, M. J. Padgett, D. J. Gauthier, and R. W. Boyd, "High-dimensional quantum cryptography with twisted light," *New J. Phys.*, vol. 17, no. 3, Mar. 2015, Art. no. 033033.
- [2] M. Mafu, A. Dudley, S. Goyal, D. Giovannini, M. McLaren, M. J. Padgett, T. Konrad, F. Petruccione, N. Lütkenhaus, and A. Forbes, "Higher-dimensional orbital-angular-momentum-based quantum key distribution with mutually unbiased bases," *Phys. Rev. A, Gen. Phys.*, vol. 88, no. 3, Sep. 2013, Art. no. 032305.
- [3] S. K. Goyal, A. H. Ibrahim, F. S. Roux, T. Konrad, and A. Forbes, "The effect of turbulence on entanglement-based free-space quantum key distribution with photonic orbital angular momentum," *J. Opt.*, vol. 18, no. 6, Apr. 2016, Art. no. 064002.
- [4] V. D'Ambrosio, F. Cardano, E. Karimi, E. Nagali, E. Santamato, L. Marrucci, and F. Sciarrino, "Test of mutually unbiased bases for six-dimensional photonic quantum systems," *Sci. Rep.*, vol. 3, Sep. 2013, Art. no. 2726.
- [5] B. Rodenburg, M. P. J. Lavery, M. Malik, M. N. O'Sullivan, M. Mirhosseini, D. J. Robertson, M. Padgett, and R. W. Boyd, "Influence of atmospheric turbulence on states of light carrying orbital angular momentum," *Opt. Lett.*, vol. 37, no. 17, pp. 3735–3737, Sep. 2012.
- [6] Y. Ren, H. Huang, G. Xie, N. Ahmed, Y. Yan, B. I. Erkmen, N. Chandrasekaran, M. P. J. Lavery, N. K. Steinhoff, M. Tur, S. Dolinar, M. Neifeld, M. J. Padgett, R. W. Boyd, J. H. Shapiro, and A. E. Willner, "Atmospheric turbulence effects on the performance of a free space optical link employing orbital angular momentum multiplexing," *Opt. Lett.*, vol. 38, no. 20, pp. 4062–4065, Oct. 2013.
- [7] Q. Tian, L. Zhu, Y. Wang, Q. Zhang, B. Liu, and X. Xin, "The propagation properties of a longitudinal orbital angular momentum multiplexing system in atmospheric turbulence," *IEEE Photon. J.*, vol. 10, no. 1, Feb. 29, 2018, Art. no. 7900416.
- [8] Y. Zhu, X. Liu, J. Gao, Y. Zhang, and F. Zhao, "Probability density of the orbital angular momentum mode of Hankel-Bessel beams in an atmospheric turbulence," *Opt. Express*, vol. 22, no. 7, pp. 7765–7772, Apr. 2014.
- [9] Y. Zhang, M. Cheng, Y. Zhu, J. Gao, W. Dan, Z. Hu, and F. Zhao, "Influence of atmospheric turbulence on the transmission of orbital angular momentum for Whittaker-Gaussian laser beams," *Opt. Express*, vol. 22, no. 18, pp. 22101–22110, Sep. 2014.
- [10] C. Paterson, "Atmospheric turbulence and orbital angular momentum of single photons for optical communication," *Phys. Rev. Lett.*, vol. 94, no. 15, Apr. 2005, Art. no. 153901.
- [11] B. Pors, C. H. Monken, E. R. Eliel, and J. P. Woerdman, "Transport of orbital-angular-momentum entanglement through a turbulent atmosphere," *Opt. Express*, vol. 19, no. 7, pp. 6671–6683, Mar. 2011.
- [12] C. Gopaul and R. Andrews, "The effect of atmospheric turbulence on entangled orbital angular momentum states," *New J. Phys.*, vol. 9, no. 4, Apr. 2007, Art. no. 94.
- [13] M. Malik, M. O'Sullivan, B. Rodenburg, M. Mirhosseini, J. Leach, M. P. J. Lavery, M. J. Padgett, and R. W. Boyd, "Influence of atmospheric turbulence on optical communications using orbital angular momentum for encoding," *Opt. Express*, vol. 20, no. 12, pp. 13195–13200, Jun. 2012.
- [14] A. H. Ibrahim, F. S. Roux, M. McLaren, T. Konrad, and A. Forbes, "Orbital-angular-momentum entanglement in turbulence," *Phys. Rev. A, Gen. Phys.*, vol. 88, no. 1, Jul. 2013, Art. no. 012312.
- [15] B. Ndagano and A. Forbes, "Characterization and mitigation of information loss in a six-state quantum-key-distribution protocol with spatial modes of light through turbulence," *Phys. Rev. A, Gen. Phys.*, vol. 98, no. 6, Dec. 2018, Art. no. 062330.
- [16] D. H. Tofsted, "Three-dimensional near-surface turbulent anisotropic structure function measurements," in *Proc. SPIE*, vol. 7685, May 2010, Art. no. 768500.
- [17] C. Robert, J.-M. Conan, V. Michau, J. Renard, C. Robert, and F. Dalaudier, "Retrieving parameters of the anisotropic refractive index fluctuations spectrum in the stratosphere from balloon-borne observations of stellar scintillation," *J. Opt. Soc. Amer. A*, vol. 25, no. 2, pp. 379–393, Feb. 2008.
- [18] C. Chen, H. Yang, S. Tong, and Y. Lou, "Two-frequency mutual coherence function for Gaussian-beam pulses propagating along a horizontal path in weak anisotropic atmospheric turbulence," *Appl. Opt.*, vol. 54, no. 18, pp. 5797–5804, Jun. 2015.
- [19] M. Beason, L. Andrews, and R. Phillips, "Study on the effect of anisotropy on a propagating beam," in *Proc. SPIE*, vol. 10408, Aug. 2017, Art. no. 104080B.
- [20] A. M. Yao and M. J. Padgett, "Orbital angular momentum: Origins, behavior and applications," *Adv. Opt. Photon.*, vol. 3, no. 2, pp. 161–204, May 2011.
- [21] I. B. Djordjevic, "Multidimensional OAM-based secure high-speed wireless communications," *IEEE Access*, vol. 5, pp. 16416–16428, 2017.
- [22] A. D. Polyani and A. V. Manzhurov, *Handbook of Mathematics for Engineers and Scientists*. Boca Raton, FL, USA: Taylor & Francis Group, 2007.
- [23] S. Mi, T. Wang, G. Jin, and C. Wang, "High-capacity quantum secure direct communication with orbital angular momentum of photons," *IEEE Photon. J.*, vol. 7, no. 5, Oct. 2015, Art. no. 7600108.



CHUNYI CHEN received the bachelor's and master's degrees in computer science and technology and the Ph.D. degree in physical electronics from the Changchun University of Science and Technology (CUST). He was a Postdoctoral Researcher with Jilin University, from January 2010 to July 2012, and a Visiting Scholar with Pennsylvania State University, from March 2013 to March 2014. He has become a Professor with CUST, since 2016. His research interests include optical wireless communications, atmospheric optical-wave propagation, information security theory, virtual reality, and so forth. He, as a reviewer, has served many academic journals, such as *Optics Letters*, *Optics Express*, *Applied Optics*, *the Journal of the Optical Communications and Networking*, *the Journal of the Optical Society of America A*, *the Journal of Optics*, *Optics and Laser Technology*, and so on.



HUAMIN YANG received the bachelor's degree in computer engineering from the Dalian University of Technology, the master's degree in computer application technology from the Jilin University of Technology, and the Ph.D. degree in optical engineering from the Changchun University of Science and Technology (CUST), where he has become a Professor, since 1999. His research interests include information transmission technology, big data, virtual reality, and so on.

...